

# Effects of axial conduction in the fluid on cryogenic regenerator performance

S. Sarangi and H.S. Baral

Cryogenic Engineering Centre, Indian Institute of Technology, Kharagpur, India

Although axial conduction in the matrix has been recognized as a major source of irreversibility in cryogenic regenerators, axial conduction in the fluid phase has largely been neglected. However, in spite of the negligible intrinsic thermal conductivity of most gases the effective conductivity of the gaseous medium in a porous bed may be quite significant, due to eddy diffusion and the consequent mixing of sections of gas at different temperatures. The governing equations of a thermal regenerator have been written in terms of the reduced length,  $\Lambda$ , reduced period,  $\Pi$ , and an axial conduction parameter,  $\lambda$ , which depends only on the void fraction and the bed length to particle diameter ratio for a flow Reynolds number  $Re > 2$ . Numerical solutions, using the finite difference technique developed by Willmott and co-workers, have been obtained for several values of the three parameters. It has been established that axial conduction in the fluid phase is important, particularly when the design reduced length  $\Lambda > 1/\lambda$ .

**Keywords:** cryogenerators; regenerators; axial conduction

A regenerator essentially consists of a porous medium called the matrix, through which a hot and a cold fluid flow alternately. The exchange of energy between the two fluid streams takes place by heat transfer from the hot fluid to the matrix and subsequent transfer to the cold fluid. This is why regenerators are often called storage-type heat exchangers, in contrast with recuperators or transfer-type heat exchangers.

Regenerative heat exchangers have been used in hot-air engines, Cowper stoves in steel making, gas turbines and air separation systems. In recent years, they have been used extensively in small cryogenic refrigerators based on the Stirling, Gifford-McMahon and similar cycles, in which they constitute the most important components. The classical design procedure for regenerators has been given by Hausen<sup>1</sup>. The effectiveness is expressed graphically in terms of two dimensionless parameters, reduced length,  $\Lambda$ , and reduced period,  $\Pi$ , defined as

$$\Lambda = \frac{hAL}{GC_p}$$

and

$$\Pi = \frac{hAP}{\rho_m C_m} \quad (1)$$

where:

$h$  = heat transfer coefficient ( $W m^{-2} K^{-1}$ )  
 $A$  = heat transfer area per unit volume ( $m^2 m^{-3}$ )  
 $L$  = length of regenerator (m)

$P$  = time period for hot/cold blow (s)  
 $G$  = fluid mass velocity ( $kg m^{-2} s^{-1}$ )  
 $\rho_m$  = density of the matrix ( $kg m^{-3}$ )  
 $C_m, C_p$  = specific heats of matrix and fluid respectively ( $J kg^{-1} K^{-1}$ )

## Ideal regenerator model

Hausen's derivation of the governing equations is based on an idealized model of the regenerator first proposed by Schumann<sup>2</sup>. This model is based on the following assumptions:

- 1 fluid flow through the regenerator is parallel and uniform throughout any cross-section;
- 2 the thermal conductivity of the matrix is zero in the direction of fluid flow and infinite perpendicular to it. Therefore, the regenerator may be characterized by the temperature profile along the flow axis, the temperature being uniform over any cross-section;
- 3 there is no conduction of heat through the fluid in the axial direction;
- 4 the convective heat transfer coefficient is constant throughout the regenerator;
- 5 the thermal properties of the fluid and the matrix materials are constant;
- 6 fluid hold-up and pressure cycling have no effect on the performance of the regenerator;
- 7 no phase change of the working fluid takes place within the regenerator;
- 8 the boundaries are adiabatic and there is no heat exchange with the surroundings;

- 9 the regenerator is in balance operation, that is,  $G_h = G_c$  and  $P_h = P_c$ ; and  
 10 regular periodic conditions have been established for all matrix elements.

In a real regenerator, however, some of these idealizations are not strictly valid, particularly assumptions 2 and 3 (above) regarding zero axial conduction through the matrix and the fluid. The significant effect of axial conduction in the matrix is particularly evident in the works of Bahnke and Howard<sup>3</sup>. They have expressed the matrix axial conduction effects in terms of a non-dimensional parameter,  $\lambda_m = k_m/(GC_p L)$ , and computed the performance of the regenerator in terms of  $\Lambda$ ,  $\Pi$  and  $\lambda_m$ . The axial conduction effects have been found to be particularly dominant at higher values of  $\Lambda$ .

### Axial conduction in the fluid phase

The effect of axial conduction in the working fluid, however, has largely been neglected in analytical studies in view of the small intrinsic (molecular) conductivity of most gases. However, when a gas flows through a packed bed there is eddy diffusion and consequent mixing of fluids in the axial direction. Just as molecular diffusion is related to molecular conductivity, eddy diffusion also causes an equivalent thermal conductivity in the axial direction. Since heat and mass transfer take place by the same mechanism, the mass diffusivity,  $D$ , and the thermal diffusivity,  $\alpha = k/\rho C_p$ , including both molecular and eddy components may be assumed to be the same quantity<sup>4</sup>. Thus, the Lewis number,  $Le = \alpha/D$ , is assumed to be unity.

The mechanism of eddy energy transport through packed beds has been extensively studied several years ago<sup>4-6</sup>. One of the most significant works in this area is that by Edwards and Richardson<sup>6</sup>. Based on extensive experimental results, they derived an empirical correlation between the longitudinal dispersion coefficient,  $D$ , and the Reynolds number,  $Re$ , as

$$Pe = [(0.38/Re) + (0.5Re/(5.0 + Re))]^{-1} \quad (2)$$

where the two dimensionless quantities,  $Re$  and  $Pe$ , are defined as

$$Re = Gd_p/\mu$$

and

$$Pe = Gd_p/\beta\rho D = Gd_p/\beta\rho\alpha = Gd_p C_p/\beta k \quad (3)$$

where:

$d_p$  = particle diameter (m)

$\mu$  = viscosity ( $\text{kg m}^{-1} \text{s}^{-1}$ )

$\beta$  = porosity (void fraction) of the matrix (dimensionless)

$k$  = equivalent thermal conductivity of the fluid ( $\text{W m}^{-1} \text{K}^{-1}$ )

$\rho$  = average fluid density ( $\text{kg m}^{-3}$ )

A plot of  $\ln(Pe)$  versus  $\ln(Re)$  shows<sup>6</sup> a power law dependence for  $Re < 2$  and a constant value of  $Pe$  ( $Pe \approx 2$ ) for  $Re > 2$ .

A dimensionless axial conduction parameter can be

defined as

$$\lambda = \frac{k}{GC_p L} = \frac{d_p}{Pe\beta L} \quad (4)$$

When the flow Reynolds number is  $> 2$ ,  $\lambda$  may be written as

$$\lambda = \frac{d_p}{2\beta L} \quad (5)$$

Thus the axial conduction parameter,  $\lambda$ , depends only on the void fraction,  $\beta$ , and the dimensionless quantity,  $L/d_p$ , when, for the fluid,  $Re > 2$ .

*Example.* Consider a cryogenic regenerator, 30 mm in diameter and 300 mm long, filled with lead balls of 1 mm diameter with a helium flow rate of  $0.1 \text{ g s}^{-1}$  at an average temperature of 40 K and 10 atm\* pressure. Using the Edwards and Richardson correlation<sup>6</sup>, we can compute the effective thermal conductivity of the fluid phase. Taking the viscosity of helium at 40 K as  $5.5 \times 10^{-6} \text{ kg m}^{-1} \text{ s}^{-1}$  (reference 7) and the porosity of a randomly packed bed of spheres as 0.39 (reference 8) we get  $Re = Gd_p/\mu = 25.7$ . Hence,  $Pe = 2$  and  $\lambda = 1/(2 \times 0.39 \times 300) = 0.0043$ .

### Mathematical model

The present regenerator model is the same as the Schumann model<sup>2</sup>, except that it excludes the assumption that there is no conduction of heat through the fluid in the axial direction i.e., in this Paper, the axial conduction in the fluid phase is considered to be finite. By considering energy conservation relations over a differential element of the regenerator, the dimensionless governing equations are derived as follows

$$\frac{\partial \theta_m}{\partial t} = \Pi(\theta_r - \theta_m) \quad (6)$$

and

$$\frac{\partial \theta_r}{\partial y} = \Lambda(\theta_m - \theta_r) + \lambda \frac{\partial^2 \theta_r}{\partial y^2} \quad (7)$$

where

$$\theta = (T - T_{ci})/(T_{hi} - T_{ci}) \quad (\text{dimensionless temperature})$$

$$y = y^*/L \quad (\text{dimensionless axial distance})$$

$$t = t^*/P \quad (\text{dimensionless time co-ordinate})$$

$T_{hi}$  and  $T_{ci}$  are the inlet temperatures of the hot and cold fluids, respectively. During the hot and cold blow periods the associated boundary and periodicity conditions are, respectively,

$$\theta_r(y = 0, t) = 1$$

and

$$\theta_r(y = 1, t) = 0$$

\*1 atm = 101 kPa

and for  $0 \leq y \leq 1$

$$\theta_m(y, t + 2) = \theta_m(y, t)$$

## Numerical solution

### Numerical scheme

Referring to the grid array shown in Figure 1 and following the method developed by Willmott<sup>9,10</sup>, Equations (6) and (7) may be put in finite difference form

$$\theta_m(i, j) = \theta_m(i, j - 1) + 0.5\Pi\Delta t[\theta_t(i, j - 1) + \theta_t(i, j) - \theta_m(i, j - 1) - \theta_m(i, j)] \quad (8)$$

and

$$\theta_t(i, j) = \theta_t(i - 1, j) + 0.5\Lambda\Delta y[\theta_m(i - 1, j) + \theta_m(i, j) - \theta_t(i - 1, j) - \theta_t(i, j)] + \frac{\lambda}{2\Delta y}[\theta_t(i - 2, j) - \theta_t(i - 1, j) - \theta_t(i, j) + \theta_t(i + 1, j)] \quad (9)$$

where  $i$  and  $j$  refer to the length and time co-ordinates, respectively, during the hot blow period. Equations (8) and (9) may be simplified to give  $\theta_m(i, j)$  and  $\theta_t(i, j)$  explicitly in the following form

$$\theta_m(i, j) = C_1\theta_m(i, j - 1) + C_2\theta_t(i, j - 1) + C_3\theta_t(i, j) \quad (10)$$

and

$$\theta_t(i, j) = D_1\theta_m(i - 1, j) + D_2\theta_m(i, j) + D_3\theta_t(i - 2, j) + D_4\theta_t(i - 1, j) + D_5\theta_t(i + 1, j) \quad (11)$$

where

$$C_1 = \left(1 - \frac{\Pi\Delta t}{2}\right) / \left(1 + \frac{\Pi\Delta t}{2}\right)$$

$$C_2 = C_3 = \frac{\Pi\Delta t}{2} / \left(1 + \frac{\Pi\Delta t}{2}\right)$$

$$D_1 = D_2 = \frac{\Lambda(\Delta y)^2}{2} / \left(\frac{\lambda}{2} + \Delta y + \frac{\Lambda(\Delta y)^2}{2}\right)$$

$$D_3 = D_5 = \frac{\lambda}{2} / \left(\frac{\lambda}{2} + \Delta y + \frac{\Lambda(\Delta y)^2}{2}\right)$$

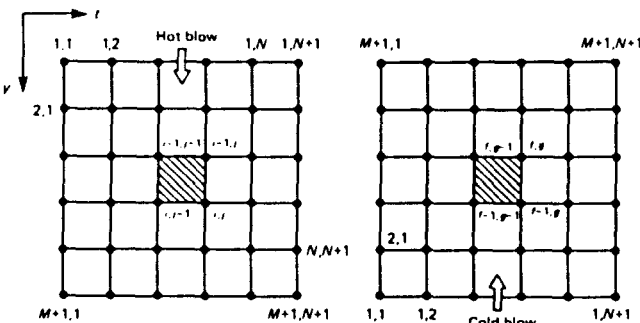


Figure 1 Grid array used in the numerical solution

and

$$D_4 = \left(\Delta y - \frac{\lambda}{2} - \frac{\Lambda(\Delta y)^2}{2}\right) / \left(\frac{\lambda}{2} + \Delta y + \frac{\Lambda(\Delta y)^2}{2}\right)$$

During the cold blow period,  $i$  and  $j$  are replaced by  $f$  and  $g$  for length and time co-ordinates, respectively,  $f$  being counted from the cold end.

The boundary and reversal conditions are now expressed as follows. Boundary conditions: during the hot blow period

$$\theta_t(1, j) = 1 \quad 1 \leq j \leq N + 1$$

and during the cold blow period

$$\theta_t(1, g) = 1 \quad 1 \leq g \leq N + 1$$

Reversal conditions: at the end of the hot blow period

$$\theta_m(f, 1) = \theta_m(M + 2 - f, N + 1)$$

and at the end of the cold blow period

$$\theta_m(i, 1) = \theta_m(M + 2 - i, N + 1)$$

Periodicity condition for all  $f$

$$\text{Abs}[\{\theta_m(f, N + 1)\}_{j_{cy}} - \{\theta_m(f, N + 1)\}_{j_{cy-1}}] < \delta$$

where  $\delta$  is an error parameter and subscripts  $cy$  and  $(cy - 1)$  refer to the present and previous cycles, respectively. While Equations (10) and (11) work well for intermediate values of  $i$ , they fail at the boundaries. In particular, it may be seen that  $\theta_t(i - 2, j)$  at  $i = 2$  and  $\theta_t(i + 1, j)$  at  $i = M + 1$  are undefined. Therefore, special forms of Equation (11) have to be used while computing  $\theta(2, j)$  and  $\theta_t(M + 1, j)$ . The finite difference form of  $(\partial^2\theta_t/\partial y^2)$  used to derive Equation (9) uses an average value of  $(\partial^2\theta_t/\partial y^2)$  between grid points  $(i, j)$  and  $(i - 1, j)$ . At the boundaries one of these terms becomes undefined. Therefore, assuming that  $(\partial^2\theta_t/\partial y^2)$  remains constant over at least one grid spacing,  $\Delta y$ , the following applies near the boundaries

$$\frac{\partial^2\theta_t}{\partial y^2} = \frac{1}{(\Delta y)^2} [\theta_t(1, j) - 2\theta_t(2, j) + \theta_t(3, j)]$$

and

$$\frac{\partial^2\theta_t}{\partial y^2} = \frac{1}{(\Delta y)^2} [\theta_t(M - 1, j) - 2\theta_t(M, j) + \theta_t(M + 1, j)]$$

for  $i = 2$  and  $M + 1$ , respectively. Thus, for points  $(2, j)$  and  $(M + 1, j)$ , Equation (11) reduces to the following special forms

$$\theta_t(2, j) = D_{1a}\theta_m(1, j) + D_{2a}\theta_m(2, j) + D_{4a}\theta_t(1, j) + D_{5a}\theta_t(3, j) \quad (11a)$$

and

$$\theta_t(M + 1, j) = D_{1b}\theta_m(M, j) + D_{2b}\theta_m(M + 1, j) + D_{3b}\theta_t(M - 1, j) + D_{4b}\theta_t(M, j) \quad (11b)$$

where

$$D_{1a} = D_{2a} = \frac{\Lambda(\Delta y)^2}{2} \left/ \left( \Delta y + \frac{\Lambda(\Delta y)^2}{2} + \frac{\lambda}{2} \right) \right.$$

$$D_{4a} = \left( \lambda + \Delta y - \frac{\Lambda(\Delta y)^2}{2} \right) \left/ \left( \Delta y + \frac{\Lambda(\Delta y)^2}{2} + \frac{\lambda}{2} \right) \right.$$

$$D_{5a} = \lambda \left/ \left( \Delta y + \frac{\Lambda(\Delta y)^2}{2} + \frac{\lambda}{2} \right) \right.$$

$$D_{1b} = D_{2b} = \frac{\Lambda(\Delta y)^2}{2} \left/ \left( \Delta y - \lambda + \frac{\Lambda(\Delta y)^2}{2} \right) \right.$$

$$D_{3b} = \lambda \left/ \left( \Delta y - \lambda + \frac{\Lambda(\Delta y)^2}{2} \right) \right.$$

$$D_{4b} = \left( \Delta y - \frac{\Lambda(\Delta y)^2}{2} - 2\lambda \right) \left/ \left( \Delta y - \lambda + \frac{\Lambda(\Delta y)^2}{2} \right) \right.$$

In the numerical solution process, Equations (11a) and (11b) replace Equation (11) while computing  $\theta_r(2, j)$  and  $\theta_r(M+1, j)$ , respectively.

### Solution procedure

Starting with an arbitrary initial matrix temperature profile, Equations (10) and (11) [or (11a) for  $i = 2$  and (11b) for  $i = M + 1$ ] are used to compute the matrix and the gas temperatures over the grid array shown in Figure 1. The initial matrix temperature profile is estimated by the following procedure. An initial estimate of the overall efficiency of the regenerator is made using Tipler's formula<sup>1</sup>

$$\varepsilon_T = \frac{\Lambda}{\Pi} \tanh\left(\frac{\Pi}{\Lambda + 2}\right) \quad (12)$$

The boundary temperatures at the start of the hot blow period are assumed to be

$$\theta_m(1, 1) = 2\varepsilon_T - 1$$

and

$$\theta_m(M+1, 1) = 0$$

A linear profile between these two boundary temperatures is assumed, thus

$$\begin{aligned} \theta_m(i, 1) &= \theta_m(1, 1) + [\theta_m(M+1, 1) - \theta_m(1, 1)](i-1)/M \\ &= (2\varepsilon_T - 1)(M+1-i)/M \end{aligned} \quad (13)$$

Starting with this initial temperature profile and the relevant boundary conditions,  $\theta_m(i, j)$  and  $\theta_r(i, j)$  are evaluated column by column.

When using Equation (11) for the evaluation of  $\theta_r(i, j)$ ,  $\theta_r(i+1, j)$  is needed. Hence, a gas temperature profile is guessed initially for each column, these are then corrected by an iterative procedure till all the  $\theta_r$  values converge within  $1 \times 10^{-5}$ . When one column is complete, the solution proceeds to the next until  $j = M + 1$ . At this point the reversal conditions are used to set the initial condition for the cold blow period. At the end of the cold blow

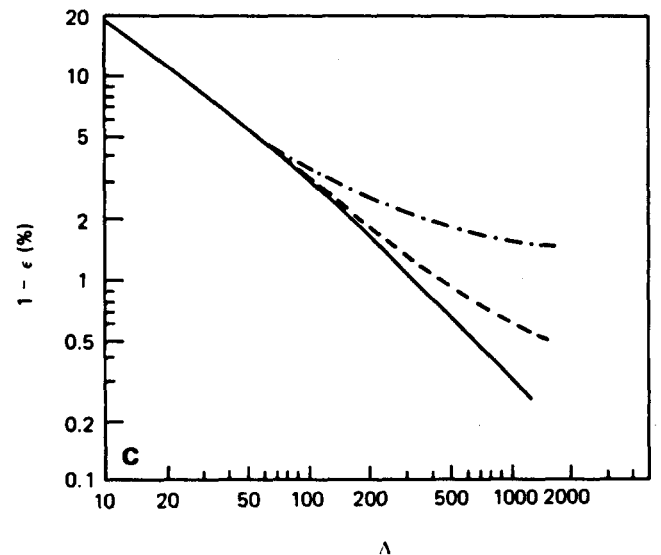
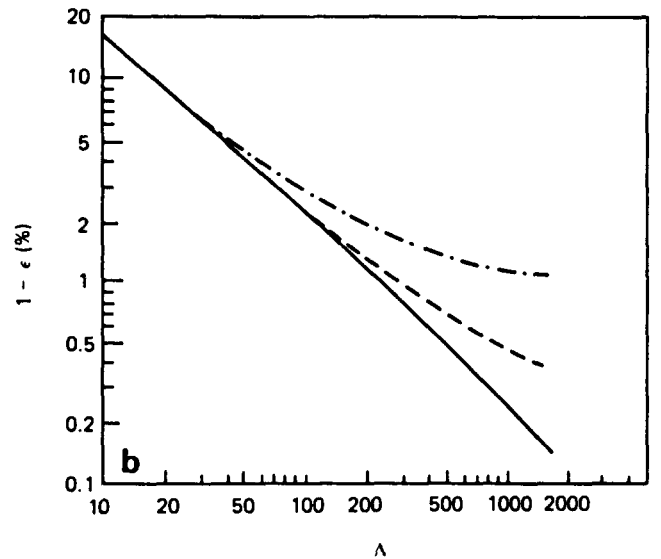
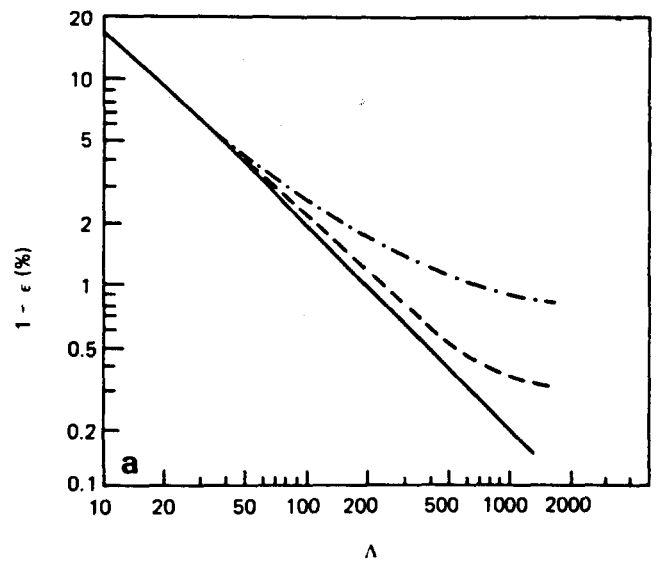


Figure 2 Ineffectiveness shown as a function of reduced length,  $\Lambda$ . (a)  $\Pi = \Lambda/8$ ; (b)  $\Pi = \Lambda/4$ ; (c)  $\Pi = \Lambda/2$ . —,  $\lambda = 0$ ; ---,  $\lambda = 0.001$ ; - · - ·,  $\lambda = 0.005$

period, reversal conditions are again used to provide the initial condition for the hot blow period.

The resulting matrix temperature profile is compared with the corresponding profile at the beginning of the previous cycle. Cyclic equilibrium is achieved when the two matrix temperature profiles agree within an error of  $1.0 \times 10^{-4}$ . Sometimes a large number of cycles are needed before equilibrium is reached. In such cases, the acceleration scheme proposed by Willmott and Kulakowski<sup>11</sup> has been used to reduce computer time. Six normal cycle calculations are performed between two acceleration steps. This eliminates the perturbations caused by the acceleration process.

When convergence is finally achieved for the entire temperature profile, the average exit temperature of the fluid over a half cycle is computed by the following formula

$$\bar{\theta}_t = \frac{1}{P} \int_0^P \theta_t(L, t) dt$$

Numerically,  $\bar{\theta}_t$  is computed by integrating  $\theta_t(M+1, j)$  using Simpson's rule. The efficiency is related to the average exit temperature by

$$\varepsilon = (1 - \bar{\theta}_t)_{\text{hot blow}} = (\bar{\theta}_t)_{\text{cold blow}}$$

## Results and discussion

Computed inefficiencies  $(1 - \varepsilon)$  have been plotted in *Figures 2a to c* against reduced length,  $\Lambda$ , for several values of reduced period,  $\Pi$  ( $\Pi = \Lambda/8, \Lambda/4$  and  $\Lambda/2$ ) and axial conduction parameter,  $\lambda$  ( $\lambda = 0, 0.001$  and  $0.005$ ). For  $\lambda = 0$ , that is, in the absence of axial conduction, the computed values are identical to those given by Hausen<sup>1</sup>. But for finite values of the axial conduction parameter,  $\lambda$ , the ineffectiveness is significantly higher. When  $\Lambda > 1/\lambda$ ,

the ineffectiveness is mainly determined by the latter parameter and is fairly independent of regenerator size, denoted by reduced length  $\Lambda$ .

Looking at the example discussed earlier, the axial conduction parameter was found to be 0.0043. Assuming  $\Lambda = 500$  and  $\Pi = \Lambda/8$ , which are quite common in cryogenic practice, from *Figure 2a* we find that the resulting ineffectiveness is almost twice that occurring in the absence of axial conduction. Thus axial conduction in the fluid phase, caused mainly by eddy diffusion, plays a significant role in high  $\Lambda$  regenerators and it should be considered along with effects such as axial conduction in the matrix, fluid hold-up and pressure cycling.

## References

- 1 Hausen, H. *Heat Transfer in Counterflow, Parallel Flow and Cross Flow* McGraw Hill, New York USA (1983)
- 2 Schumann, T.E.W. Heat transfer: a liquid flowing through a porous prism *J Franklin Inst* (1929) **208** 405-416
- 3 Bahke, G.D. and Howard, C.P. The effect of longitudinal heat conduction on periodic-flow heat exchanger performance *Trans ASME* (1964) **86-A** 105
- 4 Bernard, R.A. and Wilhelm, R.H. Turbulent diffusion in fixed beds of packed solids *Chem Eng Prog* (1950) **46(5)** 233-244
- 5 McHenry, Jr, K.W. and Wilhelm, R.H. Axial mixing of binary gas mixtures flowing in a random bed of spheres *AIChE J* (1957) **3** 83
- 6 Edwards, M.F. and Richardson, J.F. Gas dispersion in packed beds *Chem Eng Sci* (1968) **23** 109-123
- 7 Johnson, V.J. A Compendium of the properties of materials at low temperatures. Part I: Properties of Fluids, WADD Technical Report, Wright Patterson Airforce Base, USA (1960) 56-60
- 8 Haughey, D.P. and Beveridge, G.S.G. Structural properties of packed beds - a review *Can J Chem Eng* (1969) **47** 130
- 9 Willmott, A.J. Digital computer simulation of a thermal regenerator *Int J Heat Mass Transfer* (1964) **7** 1291-1302
- 10 Willmott, A.J. The regenerative heat exchanger computer representation *Int J Heat Mass Transfer* (1969) 997-1014
- 11 Willmott, A.J. and Kulakowski, B. Numerical acceleration of thermal regenerator simulation *Int J Numerical Methods Eng* (1977) **11** 533-551